

Tumor-draining lymph nodes resection and chemotherapy have diverse impacts on cancer immunotherapies

Xianda Zhao¹, Beminet Kassaye¹, Dechen Wangmo¹, Emil Lou², and Subbaya Subramanian^{1,3*}

¹Department of Surgery, University of Minnesota Medical School, Minneapolis, MN

²Department of Medicine, University of Minnesota Medical School, Minneapolis, MN

³Masonic Cancer Center, University of Minnesota, Minneapolis, MN

Running title: Effects of tumor-draining lymph nodes resection and chemotherapy on cancer immunotherapies

Keywords: immunotherapy, checkpoint inhibitors, tumor-draining lymph nodes, chemotherapy

Number of manuscript main figures: 7

Supplementary figures: 9; supplementary tables: 2

Abstract

Immunotherapies are used as adjuvant therapies for cancers after surgical resection or multiple lines of chemotherapies and or targeted therapies. Tumor-draining lymph nodes (TdLNs) are usually the first sites of metastasis; therefore, they are routinely resected for diagnostic and/ or treatment proposes. However, knowledge of how traditional cancer treatments affect immunotherapies is still very limited. Here, we present data from multiple mouse models that mimic different conditions demonstrating that TdLNs are critical for anti-tumor immunity initiation by involving tumor antigen-specific T cell priming. However, the development of immunosuppression in TdLNs and dissemination of tumor antigen-specific T cells make TdLNs less important in late-stage diseases. Removal of TdLNs concurrent with primary tumor resection did not affect immune checkpoint blockade response for localized secondary tumors. In another arm, we studied whether the timing of chemotherapy and immunotherapy in combination would affect treatment response. Using 5-fluorouracil (5-FU) cytotoxic chemotherapy as induction therapy, then followed sequentially by immune checkpoint blockade as maintenance treatment, showed better responses than adding immune checkpoint blockades concurrently with 5-FU. Immune profiling of tumors revealed that using 5-FU as an induction treatment increased tumor visibility to the immune cells, decreased immunosuppressive cells in the tumor microenvironment, and limited chemotherapy-induced T cell depletion. Collectively, our study shows the impact of TdLNs and traditional cytotoxic cancer treatment on immunotherapy response and provides essential considerations for designing successful immunotherapy strategies in complex clinical conditions.

Introduction

Immune checkpoint blockade therapies (ICBT), such as the FDA-approved anti-CTLA-4 antibody Ipilimumab, and anti-PD-1/PD-L1 antibodies Nivolumab and Atezolizumab, have transformed the therapeutic landscape of several site-specific cancer types including melanoma, and tumors of any primary site that harbor mismatch repair (MMR) deficiencies with microsatellite instability¹⁻³. Nonetheless, as with more traditional forms of systemic chemotherapy options, many patients manifest either intrinsic or acquired resistance leading to treatment failure⁴⁻⁶. Multiple mechanisms have been delineated to influence tumor response to ICBTs, including the mutational load in tumor cells, degree of T cell exhaustion, tumor microenvironmental functions, and intestinal microbiota⁴⁻⁶. In most cases, ICBT is used for treating patients with heavily pretreated tumors; thus, the interactions between first-line therapy and beyond followed by ICBTs will potentially influence tumor response to ICBTs due to tumor evolution and heterogeneity. In the case of most solid tumors, resections of non-metastatic primary tumors, with concurrent resection of draining lymph nodes, followed by administration of chemotherapies and or targeted therapies are common interventions before ICBT in most patients^{3,7,8}. However, minimal information is known about whether these interventions will impact tumors' response to ICBT.

Tumor-draining lymph nodes (TdLNs) have shown dual impacts on tumor development and treatment. On the one hand, TdLNs are critical peripheral lymphatic organs where tumor antigens are presented by dendritic cells to naïve T cells to elicit anti-tumor immunity⁹⁻¹¹. Thus, loss of TdLNs weakens immunosurveillance mechanisms, and would, therefore, promote tumor initiation⁹⁻¹². On the other hand, TdLNs are affected by tumors during tumor progression. Tumor cells release immunosuppressive factors that can be effectively drained to the TdLNs and then suppress immune cells' function¹³⁻¹⁵. Nonetheless, from a clinical standpoint, resection of TdLNs along with primary tumors comprises part of standard-of-care treatment for multiple

types of cancers. we hypothesize that this resection is an essential factor influencing long-term tumor immunity and response to ICBT.

The immunoregulatory effects of chemotherapies have been investigated in multiple cancer models with different chemotherapy drugs ¹⁶. Chemotherapy drugs, such as oxaliplatin, paclitaxel, and 5- fluorouracil have shown positive effects in anti-tumor immunity via eliciting a tumor-specific T cell response or reducing immunosuppressive factors in the tumor microenvironment ¹⁷⁻¹⁹. Bone marrow suppression is a common side effect of currently approved chemotherapies and causes leukopenia that affects anti-tumor immunity. Because chemotherapies have dual effects on regulating anti-tumor immunity, we hypothesize that the strategy of combining chemotherapy with ICBT will be critical in determining tumor response. In this study, we used 5-FU, a thymidylate synthase inhibitor that blocks DNA replication, as a representative cytotoxic chemotherapeutic drug in routine clinical use, to study the effects of chemotherapy on ICBT.

4-1BB (CD137) is an inducible co-stimulatory immune checkpoint expressed on T cells ²⁰. Unlike approved anti-CTLA-4 and anti-PD-1/PD-L1 treatments, which revive anti-tumor immunity via releasing the immunosuppressive mechanisms, anti-4-1BB (agonist) enhances anti-tumor immunity by enhancing stimulatory signals ²⁰. This distinct mechanism provided an opportunity for patients who are resistant to anti-CTLA-4 or anti-PD-1/PD-L1 therapies. Multiple 4-1BB agonists have shown promising effects in pre-clinical modes and are currently being tested in clinical trials ²¹⁻²³. Here we report our investigation of the impact of TdLNs resection and bone marrow suppressive chemotherapies in ICBT, represented by anti-4-1BB and anti-PD-1, of solid tumors in a pre-clinical mouse model of CRC.

Results

TdLNs are essential for anti-tumor immune activation and immunotherapy response in early-stage disease

To study the TdLNs, we first identified them in the subcutaneous tumor model. We injected Evans blue and Alexa Fluor 488 into tumors inoculated in the right flank of the mice to trace lymph draining (Figure S1A). 10 min to 1hr after Evans blue injection, observable staining was detected in the right inguinal and right axillary lymph nodes (Figure S1B). To develop a more sensitive detection, we used flow cytometry to trace the Alexa Fluor 488 draining in lymphatic organs for up to 48 hrs. Again, the right inguinal and right axillary lymph nodes showed the highest fluorescent intensity (Figure S1C). Other lymph nodes, such as right brachial and right popliteal lymph nodes also showed increased fluorescent signal after injection, but the signal intensity was significantly lower than in the right inguinal and right axillary lymph nodes (Figure S1C). Meanwhile, increased weight was seen in the spleen, right inguinal, and right axillary lymph nodes during tumor development, suggesting immune response happened in these lymphatic organs (Figure S2). Collectively, these results indicated that the right inguinal and right axillary lymph nodes are the sentinel TdLNs for our tumor model.

Next, we evaluated the impact of TdLNs on tumor initiation and anti-tumor immune response stimulation. Resection of TdLNs, but not non-draining lymph nodes (NdLNs), before tumor cell inoculation significantly accelerated tumor development in both CT26 and MC38 tumor models (Figure 1A). We then analyzed the stimulation of anti-tumor immunity with or without TdLNs presence. We used the frequency of tumor antigen-specific CD8⁺ T cells (10 days after tumor cells inoculation) as an indicator of anti-tumor immune response stimulation. More tumor antigen-specific CD8⁺ T cells were detected in the right and left brachial lymph nodes and spleen of tumor-bearing mice (Figure 1B). 4-1BB (CD137) provides important co-stimulatory signaling for T cells and its agonist have shown tumor eliminating effects in mice²⁰.

To test the impacts of TdLNs on immunotherapy response, we gave two injections of anti-4-1BB shortly after tumor cell inoculation to study the impact of TdLNs resection on the minimal disease. The prophylactic anti-4-1BB treatments successfully prevented tumor development in mice with intact TdLNs. Anti-tumor immunity memory was established in those tumor-free mice since they rejected the secondary tumors. However, these effects were not seen in mice with resected TdLNs (Figure 1C). These results showed that TdLNs are critical for anti-tumor immunity establishment and determine immunotherapy response in early stage disease.

TdLNs are not necessary for immunotherapy response in advanced disease tumor models

Since most TdLNs resections are performed along with primary tumor resection, we further evaluated the impact of TdLNs on tumor recurrence and response to immunotherapy in mouse models with resected primary tumors. We first allowed the primary tumor to grow to a relatively large volume and then performed primary tumor resection with or without TdLN resection. Inoculation of secondary tumors as then performed to mimic tumor recurrence (Figure 2A). Importantly, the secondary tumor growth rate was similar in mice with and without TdLNs (Figure 2A, B). In another group of TdLNs resected mice, we depleted T cells to study the impact of systemic immunity on subsequent tumor development. As expected, the secondary tumor developed the fastest in the mice with impaired systemic immunity (Figure 2A, B). As a negative control, we also included a group of mice without secondary tumor inoculation. No tumor recurrence was noticed in those mice after primary tumor resection (Table S1). TdLNs in this model were also sectioned for histology analysis, and no metastasis was found (Figure S3). Together, these results indicated that the impaired systemic immunity but not regional immunity (TdLNs resection) accelerates tumor recurrence.

Our next question is whether TdLNs resection alters immune infiltration in the secondary tumors. The major immune cell types were evaluated in the secondary tumors (Figure S4). Total tumor infiltrating T cells, PD-1 high expression T cells, and MDSCs were not changed in

secondary tumors with and without TdLNs. PD-L1 expression was also very similar. The frequency of CD103⁺ DCs and lymphatic endothelial cells were significantly higher in the secondary MC38 tumors with TdLNs (Figure S4). However, in the CT26 model, only the lymphatic endothelial cell frequency was statistically higher in secondary tumors with TdLNs than without TdLNs. The frequency of CD103⁺ DCs showed a similar trend but did not reach statistical significance (Figure S4).

Immunotherapies are usually given for patients after advanced primary tumor resection. In another pre-clinical model, we administrated anti-4-1BB and anti-PD-1 to study whether TdLNs resection will lead to immunotherapy resistance. To mimic the clinical condition, we resected the established primary tumor with or without TdLNs resection. Then, we inoculated the secondary tumor to mimic localized tumor recurrence. Shortly after the surgery, the mice were treated with anti-4-1BB or anti-PD-1 (Figure 2C). Remarkably, both anti-4-1BB and anti-PD-1 treatments were very efficient in controlling secondary tumor initiation. This effect was not abolished by TdLNs resection (Figure 2C), indicating that TdLNs resection is not a concern for immunotherapy resistance in late-stage diseases.

Immunosuppression develops in TdLNs during tumor development

Based on the above results, we then hypothesized that immunosuppression in TdLNs and systemic spreading of tumor antigen-specific T cells during tumor development make the TdLNs less important for late-stage tumors compared with early stage tumors. We collected the TdLNs and NdLNs in different stages of tumor development for analysis and compared with the naïve LNs. The frequency of CD62L⁻CD4⁺ T cells was significantly higher in TdLNs than in NdLNs when tumors are small. However, the differences disappeared once the tumors became large (Figure 3A). Also, CD80 expression is higher on antigen presentation cells in TdLNs than in NdLNs and naïve LNs only at early stage disease (Figure 3B). As the receptor of CD80, CD28 is highly expressed on CD4⁺ and CD8⁺ T cells in TdLNs of early stage tumors. The level

of CD28 expression on TdLNs T cells decreased dramatically during tumor development (Figure 3C). Previous studies indicated that CD28 is downregulated in repetitive antigen exposed T cells^{24,25}. Therefore, our observation is probably due to T cells in TdLNs of late-stage tumors are repetitively activated. However, recent studies indicated that sustained CD28 expression after T cell priming is required for T cell function and response to further stimulations, including immune checkpoint inhibitors^{26,27}. IFN- γ is highly produced by functional T cells. Decreased IFN- γ concentration was observed in TdLNs during tumor development (Figure 3D).

The amount and distribution of tumor antigen-specific T cells also influence anti-tumor immunity and immunotherapy response²⁸. Here, we measured the distribution of tumor antigen-specific T cells in mice with established tumors. As expected, the frequency of gp70 specific CD8⁺ T cells is highest in the tumor-infiltrating CD8⁺ T cells population. In other lymphatic organs, including TdLNs, NdLNs, spleen, and blood, a high frequency of gp70 specific CD8⁺ T cells were detected (Figure 3E). Some of these tumor antigen-specific T cells also expressed memory markers (Figure 3F). In summary, our results indicated that TdLNs shift from an immune active to an immunosuppressive environment during tumor development and TdLNs are not the primary reservoir of tumor antigen-specific T cells in late-stage tumors. These findings together explained why resection of TdLNs did not significantly attenuate anti-tumor immunity in late-stage disease.

Sequential treatment of 5-FU and anti-4-1BB or anti-PD-1 leads to better responses than concurrent treatment

To investigate the impact of different chemotherapy and immunotherapy combination schedules on tumor response, we performed 5-FU and anti-4-1BB or anti-PD-1 sequential treatment and concurrent treatment in mouse models. Besides, the IgG and monotherapies in immunocompetent and T cell depleted mice served as control groups (Figure 4A). In mice with established tumors, anti-4-1BB monotherapy delayed tumor growth and prolonged mice survival

time (Figure 4B, C). Anti-CD3 impaired the systemic immunity by suppressing T cell population (Figure S5). In an established tumor model, anti-CD3 pre-condition nullified the anti-tumor effects of anti-4-1BB (Figure 4B, C), indicating that an intact systemic immunity is required for anti-4-1BB response. 5-FU as effective chemotherapy also delayed tumor development in established tumor models (Figure 4B, C). Then, we added anti-4-1BB on the 5-FU treatment schedule. However, no noticeable improvement in mice survival time was observed (Figure 4B, C). In another cohort of mice, the 5-FU treatment was used as induction, and then anti-4-1BB was added as the maintenance treatment (Figure 4B, C). To determine an appropriate sequential treatment strategy, we tested the dynamic of 5-FU induced T cell depletion (Figure S5). In the sequential treatment, anti-4-1BB was given at the time when the T cell population was almost recovered from the 5-FU treatment. Tumors treated by the sequential treatment were best controlled, and the tumor-bearing mice reached the longest survival time among all groups (Figure 4B, C).

Next, we compared the 5-FU and anti-4-1BB sequential and concurrent treatments in a more clinically relevant model. In this model, we performed resection of the established primary tumor together with its TdLNs and induced secondary tumors for the treatment (Figure 5A). The sequential treatment showed better tumor suppression than concurrent treatment in a total of 60 days of experimental duration (Figure 5B). Anti-PD-1 is an FDA approved immunotherapy that has different mechanisms with anti-4-1BB. In order to test whether the conclusion from anti-4-1BB treatment is expandable, we combined 5-FU and anti-PD-1 in concurrent and sequential schedules. Again, the 5-FU and anti-PD-1 sequential treatment showed better tumor control than the concurrent treatment (Figure 5C).

Toxicity is a primary concern for cancer treatment, especially the combinational treatment. Here, we also evaluated the side effects of each treatment. The 5-FU monotherapy and 5-FU and anti-4-1BB concurrent treatment showed severe body weight loss and diarrhea

(Figure S6). In contrast, the 5-FU and anti-4-1BB sequential treatment showed slight or no side effects (Figure S6).

Sequential treatment of 5-FU and anti-4-1BB or anti-PD-1 stimulates a strong anti-tumor immune response

Our pre-clinical model suggested that the 5-FU and anti-4-1BB or anti-PD-1 sequential treatment has better tumor controlling effect than the concurrent treatment schedule. We further investigated the potential mechanisms. We performed a comprehensive immune landscape characterization in tumor tissues with 32 markers (Table S2) by mass cytometry (Figure S7). In tumor wide, CD80 and CD86 expression were upregulated in the 5-FU and anti-4-1BB sequential treatment in the CT26 tumors (Figure 6A). High expression of these two critical co-stimulatory factors suggested enhanced tumor visibility by T cells. Expression of PD-L1 and Ki-67 were not changed significantly among different groups (Figure 6A). The tumor immune infiltrations were then analyzed. Anti-4-1BB monotherapy induced tumor infiltrating T cell proliferation and increased the CD8⁺ T cell versus regulatory T cell ratio (Figure 6B, C, D). The 5-FU and anti-4-1BB sequential treatment, but not concurrent treatment, maximally reserved the positive effects of anti-4-1BB on T cell population (Figure 6B, C, D).

Meanwhile, the tumors treated by the sequential treatment had the lowest MDSCs frequency and highest NK cell frequency (Figure 6F, H). PD-1 expression on CD8⁺ T cells and macrophages frequency were similar among all groups (Figure 6E, G). The CD103⁺ DCs frequency is higher in the anti-4-1BB monotherapy group, but not statistically significant (Figure 6I). We repeated the same experiment in MC38 tumors (Figure S8) and got similar results as in CT26 tumor with most parameters. However, the CD80 and CD86 expression levels in MC38 tumors were not increased significantly by the 5-FU and anti-4-1BB sequential treatment. This difference between MC38 and CT26 tumors indicated the tumor-dependent effects of the treatment. In CT26 tumors, we also evaluated the immunoregulatory effects of 5-FU and anti-

PD-1 combination (Figure S9). The tumor wide expression of PD-L1, CD86, and CD80 was increased in the 5-FU and anti-PD-1 sequential treatment group. Meanwhile, the total T cell frequency, proliferating CD8⁺ T cell frequency, and NK cell frequency was highest in tumors treated by 5-FU and anti-PD-1 sequential treatment (Figure S9). The frequency of immunosuppressive cells, MDSCs, was decreased by the 5-FU monotherapy and combinational treatments (Figure S9). These findings pointed out that the immunological impacts of different treatment strategies and supported that 5-FU induction and anti-4-1BB or anti-PD-1 maintenance strategy has the best synergic effects in reversing the immunosuppressive tumor microenvironment.

Discussion

Immunotherapies are currently used as the second- or third-line treatments for treatment-refractory tumors. However, studies that investigate the impacts of different clinical conditions and combinational strategies on tumor immunotherapy are limited. To fill this knowledge gap, we comprehensively profiled the impacts of TdLNs resection and different chemotherapy combination schedules on immune checkpoints-based cancer therapy response.

Surgery has been the dominant treatment for several decades to prevent, diagnose, stage, and treat cancers. Radical surgery, a procedure that removes tumor blood supply, lymph nodes and sometimes adjacent structures, is routinely performed in the most common cancers, such as colorectal cancer, breast cancer, and lung cancer. Early stage cancer patients have an excellent chance to be cured by surgery alone. However, advanced diseases need more comprehensive treatments, including immunotherapies. Currently, most immunotherapies are used as adjuvant treatments, meaning that they are given after surgeries. TdLNs are the primary lymphatic organs where anti-tumor immune responses are initiated^{9-11,29,30}. In the

mouse model with resected TdLNs before tumor cell inoculation, we observed that loss of TdLNs would significantly accelerate tumor growth and compromise response to immunotherapy. These data uncovered a key role for TdLNs in preventing cancer cells from evading anti-tumor immunity in an early stage. Mechanistically, TdLNs resection in early-stage disease led to inadequate anti-tumor immunity simulation, featured with a low frequency of tumor antigen-specific T cells in lymphatic organs. Our observations were in line with previous studies, highlighting the significance of TdLNs in initiating anti-tumor immunity and regulating immunotherapy response in early-stage disease³¹.

The tumor and TdLNs two-way crosstalk remodeled each other during tumor progression^{9-11,14,15}. Immunosuppressive factors, such as TGF- β that are derived from tumors, can be drained to TdLNs for inducing an immunosuppressive microenvironment^{14,32}. In hepatocellular carcinoma patients derived samples, an immunosuppressive phenotype was observed in TdLNs as well³³. Our studies compared the immune responses in naïve LNs, TdLNs of early-stage tumors, and TdLNs of advanced tumors and showed the trend of potent immunosuppression in TdLNs during tumor progression. Although the TdLNs turned to be immunosuppressive, the distribution of tumor antigen-specific T cells is extensive in lymphatic tissues in advanced tumors. Overall, resection of TdLNs in advanced tumors did not influence secondary tumor immunity and response to immunotherapies. A recent study in early stage tumor model reported that TdLNs are determining factors of PD-1/PD-L1 immune checkpoint therapies³¹. Our study validated this conclusion, and more importantly, we tested the impacts of TdLNs on advanced tumors, which have not been studied. Our data in the advanced tumor model have valuable clinical significance since it supported the resection of TdLNs in patients that will receive immune checkpoint-based therapies as the adjuvant treatment.

Systemic therapies, such as chemotherapies, are used to shrink primary tumors, eradicate micrometastatic disease, or in widespread incurable cancers stabilize the disease³⁴.

Chemotherapies have the advantages of fast-acting and high response rate and are widely administrated as the primary treatment for combinational strategies³⁴. Combinations of chemotherapies with immunotherapies are widely discussed and currently tested in pre-clinical models and clinical trials^{17,35-37}. Mechanistically, chemotherapy can promote anti-tumor immunity via inducing immunogenic cell death and disrupting tumor microenvironment components that are used to evade the immune response³⁸⁻⁴². However, cancer chemotherapies are also considered as immune suppressive due to their cytotoxic effects on immune cells. Here, we used 5-FU, a commonly used chemotherapy drug in the past decades, as a representative to study the influences of different chemotherapy and combinational immunotherapy strategies on tumor response.

Via extensive study on the 5-FU induced immune responses, we revealed both systemic immunosuppressive effects and immune stimulating effects in the tumor microenvironment of 5-FU treatment. In the tumor microenvironment, 5-FU treatment upregulated CD80 expression and depleted MDSCs. CD80 belongs to the B7 family and is a protein found on antigen presenting cells as well as tumor cells that provides a costimulatory signal necessary for triggering T cells and natural killer cells⁴³⁻⁴⁶. Thus, upregulation of CD80 in tumor tissue induced by 5-FU treatment will potentially lead to increased tumor visibility by T cells. MDSCs are a heterogeneous population of cells that are potently suppressive to T cell responses^{47,48}. By depleting MDSCs in tumor tissue, 5-FU treatment will potentiate anti-tumor immunity by eliminating the negative regulations. Our data is in line with the previous reports⁴⁹. In addition to the immunogenic effects, we also observed that 5-FU treatment suppressed the T cell population in the tumor microenvironment. Thus, avoiding the immunosuppressive and preserving the immunogenic effects of 5-FU treatment will be the key factors that determine the response of 5-FU and immunotherapy combination.

In our study, administration of anti-4-1BB or anti-PD-1 after the 5-FU treatment induction significantly improved the tumors' response. In this combination strategy, anti-4-1BB or anti-PD-1 selectively boost T cell and NK cells response while the 5-FU treatment increases tumor visibility and suppresses MDSCs. However, when anti-4-1BB or anti-PD-1 was added to the repetitive 5-FU treatment, less synergetic effects were observed. Our data highlighted the importance of determining the best schedule for designing a successful chemo-immunotherapy combination. In addition to the time window, the dose is another potential factor that affects the chemotherapy-induced immune response. Low dose chemotherapies have shown special immunoregulatory effects in tumor models^{50,51}. Further studies are warranted to tests different chemotherapy doses on the chemo-immunotherapy combination.

In conclusion, our research investigated how traditional cancer treatments will affect the novel immunotherapies in clinically relevant tumor models. Our findings indicate that TdLNs resection has diverse impacts on anti-tumor immunity in early and advanced tumor models. Resection of TdLNs during primary tumor surgery does not induce immunosuppression or alter immunotherapy response. Meanwhile, minimizing the immunosuppressive and strengthening the immunogenic effects of traditional cancer therapies is critical for the immunotherapy induced durable cancer remission. Specifically, sequential rather than concurrent administration of cytotoxic chemotherapy followed by immunotherapy produced a significantly higher degree of anti-tumor response. These findings highlight the need for testing immunotherapies in tumor models that mimic multiple clinical conditions and provided references for designing clinical trials to determine the best cancer immunotherapy strategies.

Method

Cell cultures

Murine CRC cell lines CT26 (purchased from American Type Culture Collection (ATCC)) and MC38 (gift from Dr. Nicholas Haining) were used for the study. CT26 cells were maintained in complete RPMI-1640 medium (GIBCO BRL), supplemented with 10% heat-inactivated FBS (Thermo Fisher Scientific), 100 IU/mL penicillin, and 100 µg/mL streptomycin (Invitrogen Life Technologies). MC38 cells were cultured in the complete DMEM medium (GIBCO BRL) with the same supplements as the RPMI 1640 medium. All cells were routinely authenticated and tested for mycoplasma.

Mice

Wild type BALB/c mice (6-8 weeks old, Jackson Laboratory) and C57BL/6 mice (6-8 weeks old, Charles River Laboratories) were used for animal studies. All mice were kept in a specific pathogen-free facility with fully autoclaved cages to minimize non-tumor specific immune activation. Animal studies were approved by the institutional animal care and use committee (IACUC).

Subcutaneous tumor induction

For the subcutaneous syngeneic model, the cells were harvested at low passages, washed, and resuspended in Matrigel matrix (Corning Inc.) before injection. Mice were shaved right before injection. CT26 (2×10^5 cells/injection) or MC38 (5×10^5 cells/injection) cells were inoculated subcutaneously into the right hind-flank of 6 to 8-week-old female BALB/cJ or C57BL/6 mice. Tumor length and width were measured every three to seven days, and the volume was calculated according to the formula $(\text{length} \times \text{width}^2)/2$. Mice were divided into different experimental groups at random when tumors reached a specific size.

Identification of major tumor-draining lymph nodes

To identify the major tumor-draining lymph nodes (TdLNs), we injected 50µl 1% Evans blue (Sigma-Aldrich) or 50µl 1% Alexa Fluor® 488 dye (Thermo Fisher Scientific) into the

subcutaneous tumors (~400-500mm³). The left and right inguinal LNs, axillary LNs, brachial LNs, popliteal LNs, and mesentery LNs were taken at 10 min, 30 min, and 60 min post Evan blue injection. For the fluorescent labeled group, we collected LNs at 0.5h, 3h, 24h, and 48h post-injection. The intact LNs were visually examined for Evans blue staining. LNs, spleen, and tumor tissues were ground and meshed for single cell suspension, which is then measured by flow cytometry for Alexa Fluor® 488 dye signal. To evaluate the physical change of LNs and spleen during tumor development, we weighted LNs and spleen from naïve mice and mice with different sizes of the tumor (100-200mm³, 500-700mm³, or 1,200-1,500mm³).

Subcutaneous tumor and TdLNs resection

We resected the primary tumor when its volume reached but did not exceed 400-500mm³. The tumor-bearing mice were anesthetized with Ketamine (100 mg/kg) and Xylazine (10 mg/kg) via intraperitoneal injection. To minimize animal pain, we administrated Buprenorphine (slow-releasing, 2 mg/kg) subcutaneously 2 hours before anesthesia. Mice were prepared by removing hair from the skin region over the tumor. We prepared the skin by wiping with iodine prep pads and then alcohol prep pads. Resections were performed via elliptical incisions, 5mm left to the subcutaneous tumors. With iris scissors, we separated the capsule of subcutaneous tumors from the surrounding connective tissue to isolate and resect intact tumors. Once tumors were removed from the adjacent fascia, the incisions were sutured with 5/0 vicryl ties (polyglactin 910, Ethicon). For the TdLNs resection, the TdLNs were located based on the superficial anatomic landmark points. The mice were prepared as mentioned above. A 5-10mm incision was made and TdLNs were removed. Then the skin was sutured with 5/0 vicryl ties. For tumor re-challenge, 1 day after surgery, we inoculated the secondary tumor (CT26: 5×10^5 cells/injection, MC38: 1×10^6 cells/injection) to the surgical site to mimic tumor recurrence.

RT-qPCR

We used the murine leukemia virus envelope gp70 as a biomarker of tumor burden. Biopsies were collected from normal mouse skin, tumor tissue, and surgical margin after tumor resection. The mirVana microRNA (miRNA) Isolation Kit (Thermo Fisher Scientific) was used to extract total RNA from these biopsies. 500 ng of total RNA was used for establishing the cDNA library with the QuantiTect Reverse Transcription Kit (Qiagen). We used the LightCycler 480 Instrument (Roche Life Science) to measure 18S ribosomal RNA (rRNA) and gp70 expression. Primers used: 18S rRNA forward primer: GTTGGTTTTTCGGAAGCTGAGG, 18S rRNA reverse primer: AGTCGGCATCGTTTATGGTC, gp70 forward primer: AAAGTGACACATGCCACAA, gp70 reverse primer: CCCCAAGAGGCACAATAGAA⁵².

Flow cytometry

Flow cytometry was used to measure tumor tissue immune infiltration, tumor antigen-specific T cells, and immune cell functions. Harvested tumor tissues were chopped into small pieces (around 3 mm*3 mm) and then digested in a solution of collagenase IV (1 mg/ml) and deoxyribonuclease (DNase, 50 units/ml) at 37 °C for 1 hr with shaking. The digested tissue was then meshed and filtered through a 70 µm cell strainer. The cell suspension was centrifuged and resuspended in red blood cell lysis buffer for 15 minutes at room temperature for eliminating red blood cells. Another centrifugation was performed to get the cell pellet for staining. For the lymphatic organs, we directly meshed the tissue and filtered through a 40 µm cell strainer to get single cell suspension, followed by red blood cells elimination.

Following the tissue sample preparation, cells were stained with the fixable cell viability dye and then cell surface marker antibodies for a 15 min incubation at 4 °C. Next, cells were fixed and permeabilized for intracellular staining for a 30 min incubation at RT. The cells were finally stained with intracellular markers (30 min at RT) and analyzed on a BD FACSCANTO instrument (BD Biosciences). To analyze the tumor antigen-specific T cells, we performed H-2Ld MuLV gp70-SPSYVYHQF tetramer (MBL International) staining by following the

manufacturer's instruction, prior to antibody staining. All antibodies for flow cytometry were purchased from Biolegend and summarized in supplementary materials. Data were analyzed using the FlowJo software (Tree Star, Inc.).

Mass cytometry

Details on antibodies and reagents used are listed in supplementary table 2. We purchased the pre-labeled antibodies from Fluidigm Corporation and unlabeled antibodies (MaxPar® Ready purified) from Biolegend. Conjugation of the purified antibodies with metal tags was performed by using the MaxPar X8 antibody labeling kit (Fluidigm Corporation) according to the manufacturer's instructions. The metal tagged antibodies were then validated and titrated in positive control and negative control samples.

Tumor samples were collected and digested as the flow cytometry procedure. A total of 3 million single cells were used for each mass cytometry staining. In brief, the single cell pellets were first incubated with Cell-ID Cisplatin with a final concentration of 5 μ M for 5 min at RT to identify dead cells. Cells were then washed and blocked by Fc-receptor blocking solution. Cell membrane staining was then performed with metal-conjugated antibodies for 30 min at RT. After staining, cells were fixed and permeabilized. The intracellular staining antibodies were then added and incubated for 45 min at RT. Finally, cells were labeled with 1 ml 1,000x diluted 125 μ M Cell-ID intercalator-Ir to stain all cells in MaxPar Fix and Perm Buffer overnight at 4 °C. EQ Four Element Calibration Beads with the reference EQ passport P13H2302 were added to each staining tube right before data acquisition by a CyTOF 2 mass cytometer. The mass cytometry data were then normalized and exported for gating on alive single cells, which were then imported to the Cytobank software. A t-SNE analysis was performed with default parameters (perplexity, 30; iterations, 1,000) on all cell types in tumor samples.

Mouse IFN- γ enzyme-linked immunosorbent assays

Mouse naïve lymph nodes and TdLNs were collected, weighed, and ground in 100 μ l RIPA lysis and extraction buffer. After the tissues were lysed, the total protein was used for enzyme-linked immunosorbent assay (ELISA, Affymetrix) to detect mouse IFN- γ , by following the manufacturer's protocol.

Histology

Mouse naïve lymph nodes, TdLNs, and non-tumor draining lymph nodes (NdLNs) were collected and fixed in 10% formalin for 24 hr. Tissues were embedded in paraffin and cut for hematoxylin and eosin (H&E) staining. The whole tissue sections were scanned and analyzed for potential metastatic tumor cells.

T cell depletion

We tested the effects of 5-FU treatment and 5-FU and anti-4-1BB combinational treatment on T cell depletion *in vivo*. Intraperitoneal administration of anti-CD3 treatment (clone: 17A2, BioXcell, 5 mg/kg every 3 days) was given to induce T cell depleted mice. One dose of 5-FU (150 mg/kg) or 5-FU (150 mg/kg) and anti-4-1BB (5 mg/kg) combinational treatment was given intraperitoneally in naïve mice. Mice were sampled on day 2, 4, 7, and 9 after treatment for quantifying T cells in lymph nodes, spleen, bone marrow, and blood circulation.

Mouse treatment

Mice were treated with IgG (5 mg/kg as an anti-4-1BB control, 10 mg/kg as an anti-PD-1 control), 5-FU (150 mg/kg), anti-4-1BB agonist (5 mg/kg, clone: 3H3), or anti-PD-1 (10 mg/kg, clone: RMP1-14) for treatment purpose. For the 5-FU monotherapy, one dose of 5-FU was given every 12 days to minimize the severe side effects. For anti-4-1BB and IgG monotherapy, mice were treated every 3 days. For the 5-FU and anti-4-1BB sequential treatment, anti-4-1BB

treatment started 9 days after one dose 5-FU treatment and continued as 3 days per injection after that. For the 5-FU and anti-4-1BB concurrent treatment, we added the anti-4-1BB cycle to the 5-FU cycle. The anti-PD-1 was used as the same as the anti-4-1BB cycle. All treatments were given intraperitoneally and continued until the endpoint of study design. The treatment starting points and endpoint varied in different experiments for different purposes and were shown in the individual figure or figure legend.

5-FU toxicity evaluation

We recorded animal body weight and diarrhea score after treatments. Mice were weighed on day 12, 24, and 32 after treatment. The diarrhea score was assessed at the endpoint of each treatment by using a 4-point scoring system: 0=normal stool; 1=slight diarrhea (soft formed stool without perianal staining of the coat); 2=moderate diarrhea (unformed stool with moderate perianal staining of the coat); and 3=severe diarrhea (watery stool with severe perianal staining of the coat)⁵³.

Statistical analysis

All statistical analyses and graphing were performed using GraphPad Prism software (Version 6). Data were displayed as means \pm SEMs. For comparison of two groups quantitative data, paired or unpaired Student's t-test was performed. One-way analysis of variance (ANOVA) was utilized for multiple comparisons. Kaplan-Meier curves were plotted to visualize mouse survival, and log-rank tests were used to compare survival outcomes between subgroups. A two-tail P value of less than 0.05 was considered statistically significant.

Competing interests statement

The authors report no competing interests.

Reference

- 1 Robert, C. *et al.* Ipilimumab plus dacarbazine for previously untreated metastatic melanoma. *The New England journal of medicine* **364**, 2517-2526, doi:10.1056/NEJMoa1104621 (2011).
- 2 Topalian, S. L. *et al.* Safety, activity, and immune correlates of anti-PD-1 antibody in cancer. *The New England journal of medicine* **366**, 2443-2454, doi:10.1056/NEJMoa1200690 (2012).
- 3 Le, D. T. *et al.* Mismatch repair deficiency predicts response of solid tumors to PD-1 blockade. *Science* **357**, 409-413, doi:10.1126/science.aan6733 (2017).
- 4 Zhao, X. & Subramanian, S. Intrinsic Resistance of Solid Tumors to Immune Checkpoint Blockade Therapy. *Cancer research* **77**, 817-822, doi:10.1158/0008-5472.CAN-16-2379 (2017).
- 5 Gide, T. N., Wilmott, J. S., Scolyer, R. A. & Long, G. V. Primary and Acquired Resistance to Immune Checkpoint Inhibitors in Metastatic Melanoma. *Clinical cancer research : an official journal of the American Association for Cancer Research* **24**, 1260-1270, doi:10.1158/1078-0432.CCR-17-2267 (2018).
- 6 Sharma, P., Hu-Lieskovan, S., Wargo, J. A. & Ribas, A. Primary, Adaptive, and Acquired Resistance to Cancer Immunotherapy. *Cell* **168**, 707-723, doi:10.1016/j.cell.2017.01.017 (2017).
- 7 Lee, C. K. *et al.* Checkpoint Inhibitors in Metastatic EGFR-Mutated Non-Small Cell Lung Cancer-A Meta-Analysis. *Journal of thoracic oncology : official publication of the International Association for the Study of Lung Cancer* **12**, 403-407, doi:10.1016/j.jtho.2016.10.007 (2017).
- 8 Rizvi, N. A. *et al.* Activity and safety of nivolumab, an anti-PD-1 immune checkpoint inhibitor, for patients with advanced, refractory squamous non-small-cell lung cancer (CheckMate 063): a phase 2, single-arm trial. *The Lancet. Oncology* **16**, 257-265, doi:10.1016/S1470-2045(15)70054-9 (2015).
- 9 Fisher, B. & Fisher, E. R. Studies concerning the regional lymph node in cancer. I. Initiation of immunity. *Cancer* **27**, 1001-1004 (1971).
- 10 Munn, D. H. & Mellor, A. L. The tumor-draining lymph node as an immune-privileged site. *Immunological reviews* **213**, 146-158, doi:10.1111/j.1600-065X.2006.00444.x (2006).
- 11 Shu, S., Cochran, A. J., Huang, R. R., Morton, D. L. & Maecker, H. T. Immune responses in the draining lymph nodes against cancer: implications for immunotherapy. *Cancer metastasis reviews* **25**, 233-242, doi:10.1007/s10555-006-8503-7 (2006).
- 12 Karlsson, M. *et al.* Pilot study of sentinel-node-based adoptive immunotherapy in advanced colorectal cancer. *Annals of surgical oncology* **17**, 1747-1757, doi:10.1245/s10434-010-0920-8 (2010).
- 13 Cochran, A. J. *et al.* Sentinel lymph nodes show profound downregulation of antigen-presenting cells of the paracortex: implications for tumor biology and treatment. *Modern pathology : an official journal of the United States and Canadian Academy of Pathology, Inc* **14**, 604-608, doi:10.1038/modpathol.3880358 (2001).
- 14 Ito, M. *et al.* Tumor-derived TGFbeta-1 induces dendritic cell apoptosis in the sentinel lymph node. *Journal of immunology* **176**, 5637-5643, doi:10.4049/jimmunol.176.9.5637 (2006).
- 15 Watanabe, S. *et al.* Tumor-induced CD11b+Gr-1+ myeloid cells suppress T cell sensitization in tumor-draining lymph nodes. *Journal of immunology* **181**, 3291-3300, doi:10.4049/jimmunol.181.5.3291 (2008).
- 16 Bracci, L., Schiavoni, G., Sistigu, A. & Belardelli, F. Immune-based mechanisms of cytotoxic chemotherapy: implications for the design of novel and rationale-based combined treatments against cancer. *Cell death and differentiation* **21**, 15-25, doi:10.1038/cdd.2013.67 (2014).
- 17 Pfirschke, C. *et al.* Immunogenic Chemotherapy Sensitizes Tumors to Checkpoint Blockade Therapy. *Immunity* **44**, 343-354, doi:10.1016/j.immuni.2015.11.024 (2016).

- 18 Khosravianfar, N. *et al.* Myeloid-derived Suppressor Cells Elimination by 5-Fluorouracil Increased Dendritic Cell-based Vaccine Function and Improved Immunity in Tumor Mice. *Iranian journal of allergy, asthma, and immunology* **17**, 47-55 (2018).
- 19 Zhang, L. *et al.* Differential impairment of regulatory T cells rather than effector T cells by paclitaxel-based chemotherapy. *Clinical immunology* **129**, 219-229, doi:10.1016/j.clim.2008.07.013 (2008).
- 20 Chester, C., Ambulkar, S. & Kohrt, H. E. 4-1BB agonism: adding the accelerator to cancer immunotherapy. *Cancer immunology, immunotherapy : CII* **65**, 1243-1248, doi:10.1007/s00262-016-1829-2 (2016).
- 21 Buchan, S. L. *et al.* Antibodies to Costimulatory Receptor 4-1BB Enhance Anti-tumor Immunity via T Regulatory Cell Depletion and Promotion of CD8 T Cell Effector Function. *Immunity* **49**, 958-970 e957, doi:10.1016/j.immuni.2018.09.014 (2018).
- 22 Shindo, Y. *et al.* Combination immunotherapy with 4-1BB activation and PD-1 blockade enhances antitumor efficacy in a mouse model of subcutaneous tumor. *Anticancer research* **35**, 129-136 (2015).
- 23 Segal, N. H. *et al.* Results from an Integrated Safety Analysis of Urelumab, an Agonist Anti-CD137 Monoclonal Antibody. *Clinical cancer research : an official journal of the American Association for Cancer Research* **23**, 1929-1936, doi:10.1158/1078-0432.CCR-16-1272 (2017).
- 24 Vallejo, A. N., Brandes, J. C., Weyand, C. M. & Goronzy, J. J. Modulation of CD28 expression: distinct regulatory pathways during activation and replicative senescence. *Journal of immunology* **162**, 6572-6579 (1999).
- 25 Lake, R. A., O'Hehir, R. E., Verhoef, A. & Lamb, J. R. CD28 mRNA rapidly decays when activated T cells are functionally anergized with specific peptide. *International immunology* **5**, 461-466, doi:10.1093/intimm/5.5.461 (1993).
- 26 Linterman, M. A. *et al.* CD28 expression is required after T cell priming for helper T cell responses and protective immunity to infection. *eLife* **3**, doi:10.7554/eLife.03180 (2014).
- 27 Kamphorst, A. O. *et al.* Rescue of exhausted CD8 T cells by PD-1-targeted therapies is CD28-dependent. *Science* **355**, 1423-1427, doi:10.1126/science.aaf0683 (2017).
- 28 Liu, J. *et al.* Improved Efficacy of Neoadjuvant Compared to Adjuvant Immunotherapy to Eradicate Metastatic Disease. *Cancer discovery* **6**, 1382-1399, doi:10.1158/2159-8290.CD-16-0577 (2016).
- 29 Marzo, A. L. *et al.* Tumor antigens are constitutively presented in the draining lymph nodes. *Journal of immunology* **162**, 5838-5845 (1999).
- 30 Jeanbart, L. *et al.* Enhancing efficacy of anticancer vaccines by targeted delivery to tumor-draining lymph nodes. *Cancer immunology research* **2**, 436-447, doi:10.1158/2326-6066.CIR-14-0019-T (2014).
- 31 Fransen, M. F. *et al.* Tumor-draining lymph nodes are pivotal in PD-1/PD-L1 checkpoint therapy. *JCI insight* **3**, doi:10.1172/jci.insight.124507 (2018).
- 32 Cochran, A. J. *et al.* Tumour-induced immune modulation of sentinel lymph nodes. *Nature reviews. Immunology* **6**, 659-670, doi:10.1038/nri1919 (2006).
- 33 Shuang, Z.-Y. *et al.* The tumor-draining lymph nodes are immunosuppressed in patients with hepatocellular carcinoma. *Translational Cancer Research* **6**, 1188-1196 (2017).
- 34 DeVita, V. T., Jr. & Chu, E. A history of cancer chemotherapy. *Cancer research* **68**, 8643-8653, doi:10.1158/0008-5472.CAN-07-6611 (2008).
- 35 Kareva, I. A Combination of Immune Checkpoint Inhibition with Metronomic Chemotherapy as a Way of Targeting Therapy-Resistant Cancer Cells. *International journal of molecular sciences* **18**, doi:10.3390/ijms18102134 (2017).
- 36 Emens, L. A. & Middleton, G. The interplay of immunotherapy and chemotherapy: harnessing potential synergies. *Cancer immunology research* **3**, 436-443, doi:10.1158/2326-6066.CIR-15-0064 (2015).

- 37 Wang, N., Wang, Z., Xu, Z., Chen, X. & Zhu, G. A Cisplatin-Loaded Immunochemotherapeutic Nanohybrid Bearing Immune Checkpoint Inhibitors for Enhanced Cervical Cancer Therapy. *Angewandte Chemie* **57**, 3426-3430, doi:10.1002/anie.201800422 (2018).
- 38 Galluzzi, L., Buque, A., Kepp, O., Zitvogel, L. & Kroemer, G. Immunogenic cell death in cancer and infectious disease. *Nature reviews. Immunology* **17**, 97-111, doi:10.1038/nri.2016.107 (2017).
- 39 Samanta, D. *et al.* Chemotherapy induces enrichment of CD47(+)/CD73(+)/PDL1(+) immune evasive triple-negative breast cancer cells. *Proceedings of the National Academy of Sciences of the United States of America* **115**, E1239-E1248, doi:10.1073/pnas.1718197115 (2018).
- 40 Lutsiak, M. E. *et al.* Inhibition of CD4(+)²⁵⁺ T regulatory cell function implicated in enhanced immune response by low-dose cyclophosphamide. *Blood* **105**, 2862-2868, doi:10.1182/blood-2004-06-2410 (2005).
- 41 Michels, T. *et al.* Paclitaxel promotes differentiation of myeloid-derived suppressor cells into dendritic cells in vitro in a TLR4-independent manner. *Journal of immunotoxicology* **9**, 292-300, doi:10.3109/1547691X.2011.642418 (2012).
- 42 Tesniere, A. *et al.* Immunogenic death of colon cancer cells treated with oxaliplatin. *Oncogene* **29**, 482-491, doi:10.1038/onc.2009.356 (2010).
- 43 Lanier, L. L. *et al.* CD80 (B7) and CD86 (B70) provide similar costimulatory signals for T cell proliferation, cytokine production, and generation of CTL. *Journal of immunology* **154**, 97-105 (1995).
- 44 Chambers, B. J., Salcedo, M. & Ljunggren, H. G. Triggering of natural killer cells by the costimulatory molecule CD80 (B7-1). *Immunity* **5**, 311-317 (1996).
- 45 Singh, N. P. *et al.* A novel approach to cancer immunotherapy: tumor cells decorated with CD80 generate effective antitumor immunity. *Cancer research* **63**, 4067-4073 (2003).
- 46 Beyranvand Nejad, E. *et al.* Tumor Eradication by Cisplatin Is Sustained by CD80/86-Mediated Costimulation of CD8⁺ T Cells. *Cancer research* **76**, 6017-6029, doi:10.1158/0008-5472.CAN-16-0881 (2016).
- 47 Kumar, V., Patel, S., Tcyganov, E. & Gabrilovich, D. I. The Nature of Myeloid-Derived Suppressor Cells in the Tumor Microenvironment. *Trends in immunology* **37**, 208-220, doi:10.1016/j.it.2016.01.004 (2016).
- 48 Veglia, F., Perego, M. & Gabrilovich, D. Myeloid-derived suppressor cells coming of age. *Nature immunology* **19**, 108-119, doi:10.1038/s41590-017-0022-x (2018).
- 49 Vincent, J. *et al.* 5-Fluorouracil selectively kills tumor-associated myeloid-derived suppressor cells resulting in enhanced T cell-dependent antitumor immunity. *Cancer research* **70**, 3052-3061, doi:10.1158/0008-5472.CAN-09-3690 (2010).
- 50 Ghiringhelli, F. *et al.* Metronomic cyclophosphamide regimen selectively depletes CD4⁺CD25⁺ regulatory T cells and restores T and NK effector functions in end stage cancer patients. *Cancer immunology, immunotherapy : CII* **56**, 641-648, doi:10.1007/s00262-006-0225-8 (2007).
- 51 Cao, Z. *et al.* Antitumor and immunomodulatory effects of low-dose 5-FU on hepatoma 22 tumor-bearing mice. *Oncology letters* **7**, 1260-1264, doi:10.3892/ol.2014.1856 (2014).
- 52 Scrimieri, F. *et al.* Murine leukemia virus envelope gp70 is a shared biomarker for the high-sensitivity quantification of murine tumor burden. *Oncoimmunology* **2**, e26889, doi:10.4161/onci.26889 (2013).
- 53 Song, M. K., Park, M. Y. & Sung, M. K. 5-Fluorouracil-induced changes of intestinal integrity biomarkers in BALB/c mice. *Journal of cancer prevention* **18**, 322-329 (2013).

Figure legends

Figure 1. Impacts of TdLNs on tumor initiation and immunotherapy response in early stage tumor models.

A. Experimental schedule and tumor growth curves in mice with or without TdLNs. Both CT26 subcutaneous model (Bab/c mouse as the host) and MC38 subcutaneous model (C57BL/6 mouse as the host) were enrolled in the experiment. Mice were pre-conditioned by TdLNs resection (right inguinal and axillary LNs), NdLNs resection (left inguinal and axillary LNs), or sham surgery prior to tumor inoculation. Accelerated tumor growth was observed in mice without TdLNs (n=5 in each group). **B.** Distribution of tumor antigen (gp70) specific CD8⁺ T cells in tumor bearing mice with or without TdLNs. Less tumor antigen specific CD8⁺ T cells was detected in right and left brachial lymph nodes and spleen of TdLNs resected tumor bearing mice (n=4 in each group). **C.** Experimental schedule and early stage tumor response to anti-4-1BB treatment. Two injections of anti-4-1BB were given shortly after tumor inoculation. The treatment prevented tumor development in tumor bearing mice with intact TdLNs. Re-challenge of the tumor cells didn't form tumors in all anti-4-1BB cured mice. Data were displayed as means ± SEMs, NS: no significance, * $p < 0.05$, ** $p < 0.001$, *** $p < 0.001$ for all plots.

Figure 2. Impact of TdLNs on tumor recurrence and immunotherapy response in advanced stage tumor models.

A. The experimental schedule was showed at the top. Resection of TdLNs didn't accelerate localized secondary tumor development in both CT26 and MC38 subcutaneous tumor models. However, systemic deletion of T cells significantly accelerated secondary tumor development in both tumor models (n=8-10 in each group). **B.** Systemic depletion of T cells, but not TdLNs

resection, led to a shorter survival time of mice due to secondary tumor development (n=8-10 in each group, log-rank test $p<0.01$). **C.** Response to anti-4-1BB and anti-PD-1 treatment was tested in localized secondary tumors with or without TdLNs. Anti-4-1BB and anti-PD-1 treatment suppressed secondary tumor growth in both TdLN intact and resected mice. However, anti-4-1BB treatment lost its anti-tumor activity in mice with impaired systemic T cell response (n=5 in each group). Data were displayed as means \pm SEMs for all plots.

Figure 3. Immunosuppression in TdLNs and tumor antigen specific T cell distribution in tumor bearing mice with advanced disease.

A. More activated (CD62L⁻) CD4⁺ T cells were observed in TdLNs than NdLNs on 7 days post tumor cells inoculation. However, at the late stage of tumor development, the proportion of activated CD4⁺ T cells were similar in TdLNs and NdLNs. The proportion of activated CD8⁺ T cells were close in TdLNs and NdLNs during tumor development (n=4 in each group). **B.** CD80 expression level on antigen presentation cells (APCs) was higher in TdLNs than NdLNs on 7 days post tumor cells inoculation (n=4 in each group). **C.** The proportion of CD28⁺ T cells (both CD4⁺ and CD8⁺) in TdLNs were decreased during tumor development (n=4 in each group). **D.** Concentration of IFN- γ in TdLNs was higher at the early stage of tumor development than the late stage (n=4 in each group). **E.** At the late stage of tumor development, systemic distribution of tumor antigen (gp70) specific CD8⁺ T cells was detected in multiple lymphatic organs and the tumor microenvironment. The tumor microenvironment has the highest frequency of gp70 specific CD8⁺ T cells than lymphatic organs (n=3 in each group). **F.** Memory phenotype of gp70 specific CD8⁺ T cells were detected in multiple lymphatic organs and tumor microenvironment (n=3 in each group). Data were displayed as means \pm SEMs, * $p<0.05$, ** $p<0.01$, *** $p<0.001$, **** $p<0.0001$ for all plots.

Figure 4. 5-FU and anti-4-1BB sequential treatment elicits strong anti-tumor activity.

A. Tumor (500mm³ to 700mm³ in volume) bearing mice were randomly assigned to 6 treatment groups: IgG (one dose/3 days), 5-FU monotherapy (one dose/12 days), anti-4-1BB monotherapy (one dose/3 days), anti-CD3 therapy (one dose/3 days) and anti-4-1BB therapy (one dose/3 days, two days after anti-CD3), 5-FU (one dose) and anti-4-1BB (1 dose/3 days, started at 9 days post 5-FU) sequential therapy, and 5-FU (one dose/12 days) and anti-4-1BB (1 dose/3 days, started at the same day of 5-FU) concurrent therapy. The treatment was continued until the endpoint of follow-up. **B.** CT26 tumor response to different treatments. The 5-FU and anti-4-1BB sequential treatment significantly prolonged survival time of the tumor bearing mice (n=4 in each group for the tumor growth curve, n=7 in each group for the mouse survival curve, log-rank test $p<0.01$). **C.** The same experiments were repeated in MC38 tumor model (n=4 in each group for the tumor growth curve, n=7 in each group for the mouse survival curve, log-rank test $p<0.01$). Data were displayed as means \pm SEMs for all plots.

Figure 5. 5-FU and anti-4-1BB sequential treatment on secondary tumors that mimic tumor recurrence.

A. The primary tumor and TdLNs were resected when tumors are at 400mm³-500mm³ in volume. Secondary tumors were induced and treated by different strategies at 300mm³-350mm³ in volume. **B-C.** The 5-FU and anti-4-1BB or anti-PD-1 sequential treatment was more efficient than the 5-FU and anti-4-1BB or anti-PD-1 concurrent treatment in controlling secondary tumors in CT26 and MC38 models (n=7 in each group, * $p<0.05$). Data were displayed as means \pm SEMs for all plots.

Figure 6. Tumor immunological response to 5-FU and anti-4-1BB treatments in CT26 tumors.

A. ViSNE plot showed single cell level expression of PD-L1, Ki-67, CD80, and CD86 in the tumor tissue. **B.** PD-L1, Ki-67, CD80, and CD86 expression were quantified in whole tumor tissue. The 5-FU and anti-4-1BB sequential treatment significantly upregulated CD86 and CD80 expression in tumor tissues (n=3 in each group). **C-J.** The tumor infiltrating T cell frequency, CD8/Treg ratio, Ki-67⁺ CD8⁺ T cell frequency, expression of PD-1 on CD8⁺ T cell, myeloid derived suppressive cells (MDSCs) frequency, macrophages frequency, NK cells frequency, and CD103⁺ dendritic cells (DCs) frequency were measured in tumors treated by different strategies. The 5-FU and anti-4-1BB sequential treatment was compared with the anti-4-1BB monotherapy, 5-FU monotherapy, and 5-FU and anti-4-1BB concurrent treatment (n=3 in each group). Data were displayed as means \pm SEMs, NS: no significance, * p <0.05, ** p <0.001, *** p <0.001 for all plots.

Figure 7. Graphic abstract.

The effects of tumor draining lymph nodes (TdLNs) resection and combination of cytotoxic chemotherapy on immune checkpoint blockade therapies are evaluated in this study. Resection of TdLNs shows different impacts on early and late stage tumor models. Meanwhile, the sequential combination of cytotoxic chemotherapy and immunotherapy shows better tumor control than concurrent combination.

Supplementary Figure legends:

Supplementary figure 1. Identification of tumor draining lymph nodes (TdLNs) in mouse.

A. Evan blue dye or Alexa Fluor[®] 488 dye was injected into the tumor in the right hinge flank to trace TdLNs. **B.** 10 min post Evan blue dye injection, the right inguinal (RI) and right axillary (RA) lymph nodes (LNs) were obviously stained. Deeper color was seen at 30 min and 60 min post injection. The representative data of three independent experiments were shown. **C.** Flow cytometry was used for detecting the Alexa Fluor[®] 488 dye distribution in lymphatic organs. The RI LN and RA LN showed the highest FITC signal and were identified as the major TdLNs. The other LNs were identified as the non-draining lymph nodes (NdLNs) (n=3 in each group). Data were displayed as means \pm SEMs for all plots.

Supplementary figure 2. Physical changes of TdLNs, NdLNs, and spleen of tumor bearing mice.

The weight of spleen, and major superficial LNs (both TdLNs and NdLNs) was measured at different time points of tumor development. **A.** During tumor development, significant splenomegaly was observed (n=4 in each group). **B-J.** Obvious lymphadenopathy was observed in the TdLNs rather than in the NdLNs during tumor development (n=4 in each group). Data were displayed as means \pm SEMs, * p <0.05, ** p <0.001, *** p <0.001 for all plots.

Supplementary figure 3. Histology of naive LNs, TdLNs and NdLNs.

At the late stage of tumor development, the histology of TdLNs and NdLNs was evaluated. The TdLNs were larger than NdLNs and naïve LNs (taken from tumor-free mice). No metastasis was observed in TdLNs. Representative data from three independent experiments was shown.

Supplementary figure 4. Immune features in secondary tumors with or without TdLNs.

A. The frequency of lymphatic endothelia cells was higher in CT26 secondary tumors with TdLNs than secondary tumors without TdLNs (n=8 in each group). The total tumor infiltrating T-cell frequency, PD-1 high expression T-cells frequency, CD103⁺ dendritic cells (DCs) frequency, myeloid derived suppressive cells (MDSCs) frequency, and PD-L1 expression were similar in two groups (n=4 in each group). **B.** The experiments were repeated in the MC38 tumor model. The frequency of lymphatic endothelia cells and CD103⁺ DCs were higher in secondary tumors with TdLNs than in secondary tumors without TdLNs (n=4 in each group). Data were displayed as means \pm SEMs, NS: no significance, * p <0.05 for all plots.

Supplementary figure 5. T-cell depleting effects of 5-FU and anti-CD3 treatment.

A. 5-FU treatment on naïve mice depleted T-cells in lymphatic organs, blood circulation, and bone marrow. The T-cell population was recovered around 9 days after 5-FU treatment. **B.** Single dose of anti-CD3 treatment on naïve mice depleted T-cells for around 3 days. **C-D.** Combination of anti-4-1BB with 5-FU didn't rescue the T-cell depletion induced by 5-FU treatment (n=3 in each group, NS: no significance). Data were displayed as means \pm SEMs for all plots.

Supplementary figure 6. Side effects of different treatments.

A-B. The mouse body weight was measured on day 12, 24, and 32 during treatment (related to figure 4). On day 32, the mice treated with the 5-FU and anti-4-1BB sequential treatment have higher body weight than the mice treated with the 5-FU and anti-4-1BB concurrent treatment (n=7 in each group, **** p <0.0001). **C-D.** Diarrhea assessment was performed at the endpoint of mice follow-up to evaluate the side effects on mouse intestine. The 5-FU and anti-4-1BB concurrent but not sequential treatment

caused severe diarrhea (n=7 in each group, **** $p<0.0001$). Data were displayed as means \pm SEMs for all plots.

Supplementary figure 7. Gating of the tumor infiltrating immune cells.

A. The major tumor infiltrating immune cell populations were showed in the tSNE plots. **B.** Manual gating of the major tumor infiltrating immune cells. The alive cell population was first identified and the immune cells (CD45+) were then gated. The gating of T-cell populations (CD45⁺CD3⁺CD8⁺ for CD8⁺T-cells, CD45⁺CD3⁺CD4⁺CD25⁺Foxp3⁺ for Tregs), NK cells (CD45⁺CD3⁻CD11b⁻CD11c⁻CD49b⁺), macrophages (CD45⁺CD3⁻CD11b⁺F4/80⁺), myeloid derived suppressive cells (MDSCs, CD45⁺CD3⁻CD11b⁺Gr-1⁺), and CD103⁺ DCs (CD45⁺CD3⁻CD11b⁻CD11c⁺I-A/I-E⁺CD103⁺) were showed here. The same markers were used throughout the study to identify the immune cells.

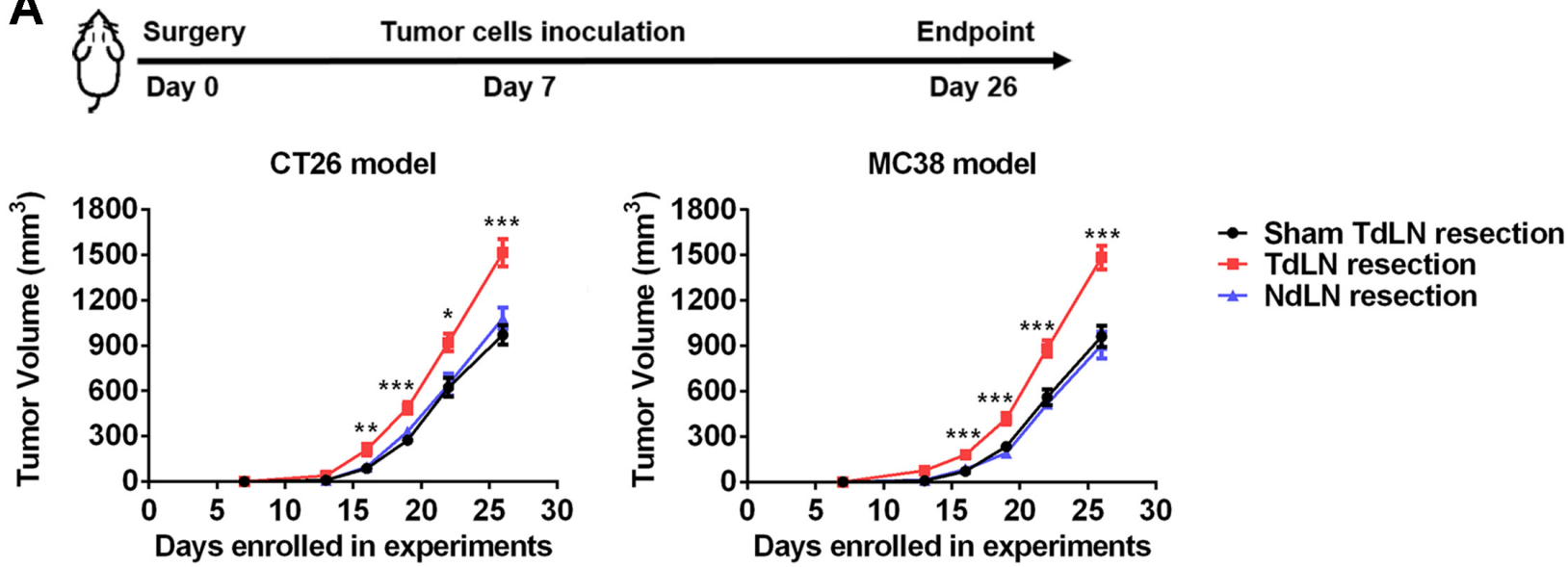
Supplementary figure 8. Tumor immunological response to 5-FU and anti-4-1BB treatments in MC38 tumors.

A. ViSNE plot showed single cell level expression of PD-L1, Ki-67, CD80, and CD86 in the MC38 tumor tissue. **B.** The 5-FU and anti-4-1BB sequential treatment significantly upregulated CD80 while decreased Ki-67 expression in tumor tissues (n=4 in each group). **C-J.** The tumor infiltrating T-cell frequency, CD8/Treg ratio, and Ki-67⁺ CD8⁺ T-cell frequency were higher in the sequential treatment than the concurrent treatment group. The myeloid derived suppressive cells (MDSCs) was depleted in 5-FU treated groups. The 5-FU and anti-4-1BB sequential treatment was compared with the anti-4-1BB monotherapy, 5-FU monotherapy, and 5-FU and anti-4-1BB concurrent treatment (n=4 in each group). Data were displayed as means \pm SEMs, NS: no significance, * $p<0.05$, ** $p<0.001$, *** $p<0.001$ for all plots.

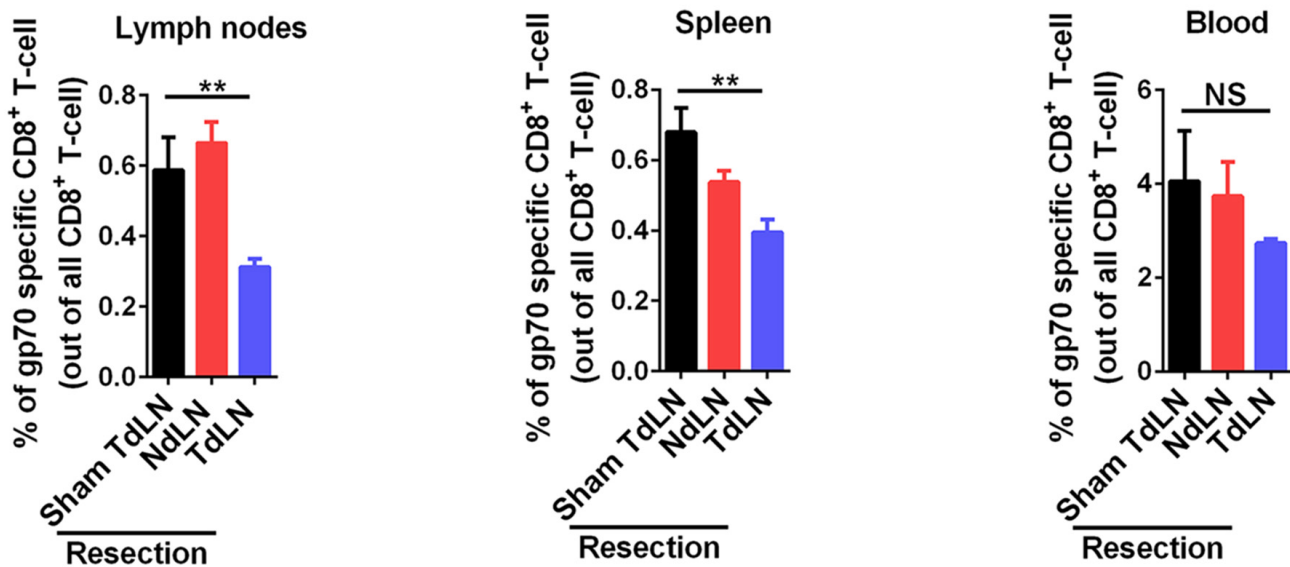
Supplementary figure 9. Tumor immunological response to 5-FU and anti-PD-1 treatments in CT26 tumors.

A-D. The 5-FU and anti-PD-1 sequential treatment significantly increased PD-L1, CD80, and CD86 expression in CT26 tumors (n=5 in each group). **E-H.** The 5-FU and anti-PD-1 sequential treatment significantly increased tumor infiltrating T-cell frequency, Ki-67⁺ CD8⁺ T-cell frequency, and NK cells frequency in tumor tissues, compared with the concurrent treatment. The myeloid derived suppressive cells (MDSCs) was depleted in 5-FU treated groups (n=5 in each group). Data were displayed as means \pm SEMs, NS: no significance, * p <0.05, ** p <0.001, *** p <0.001 for all plots.

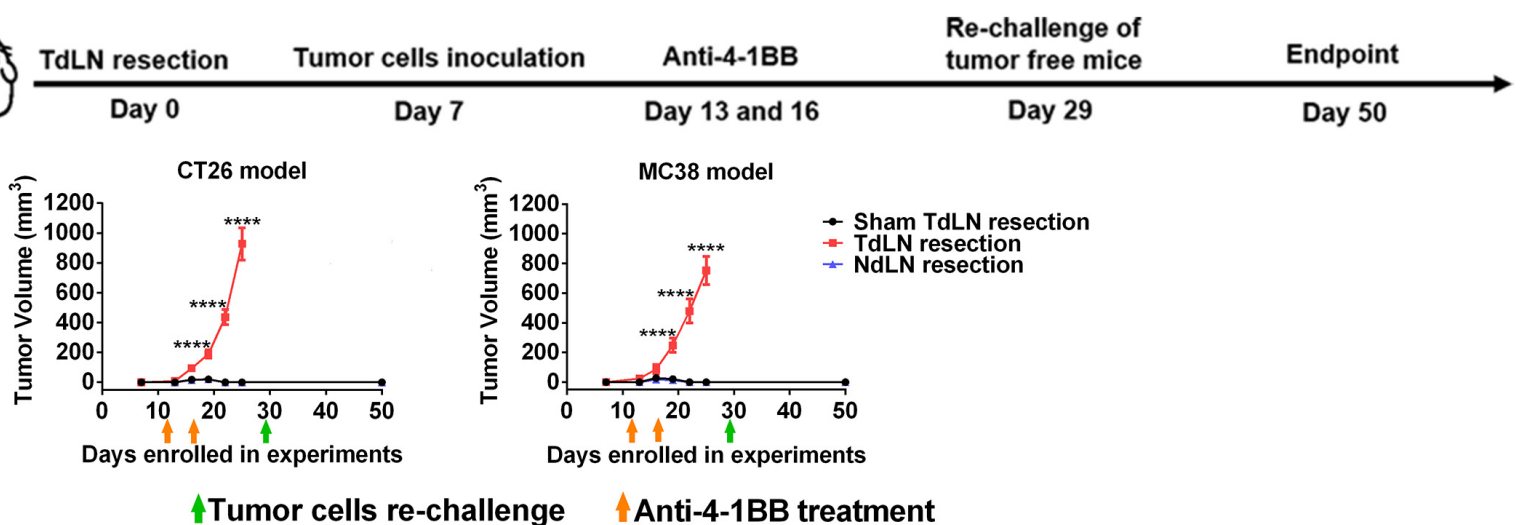
A

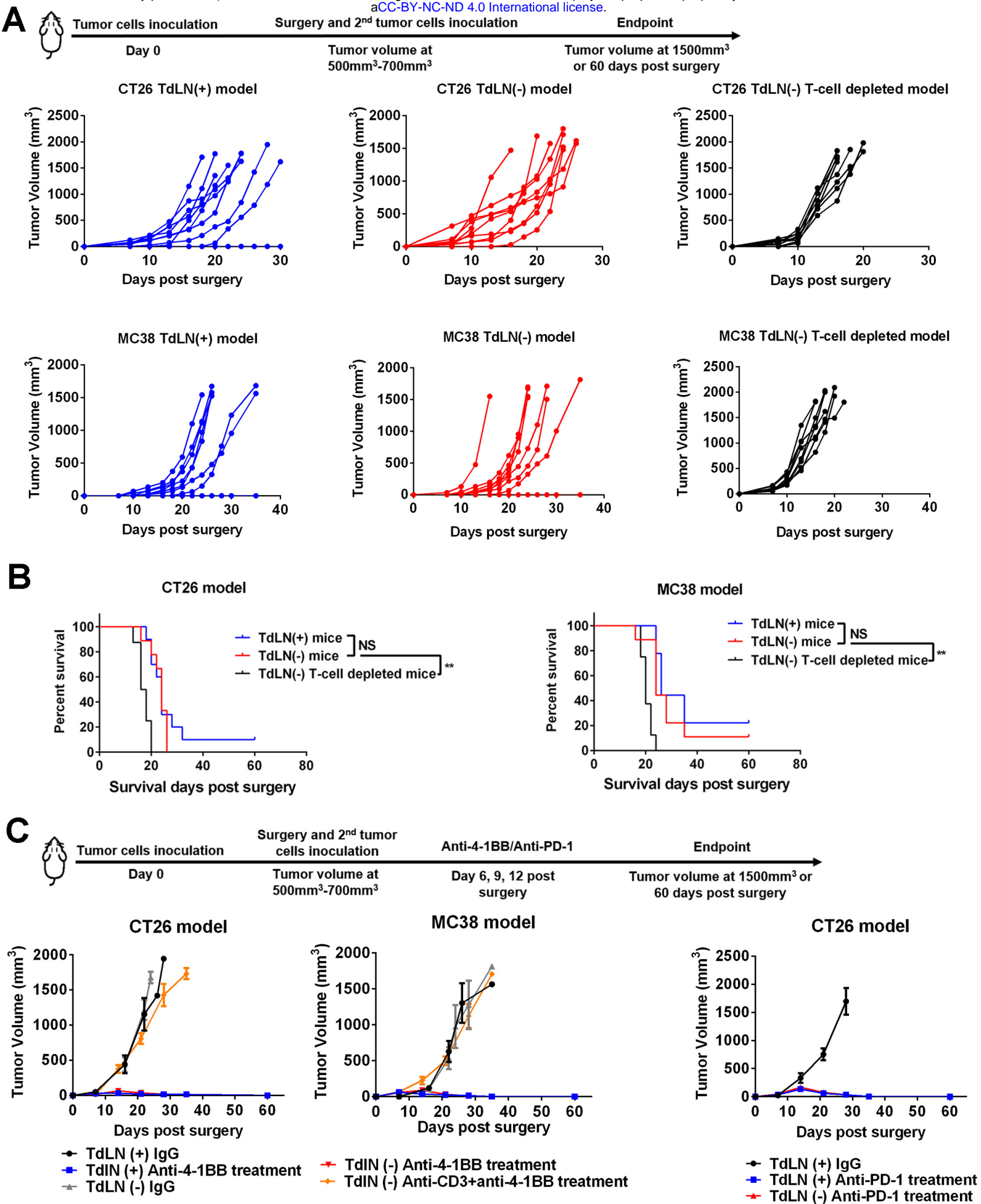


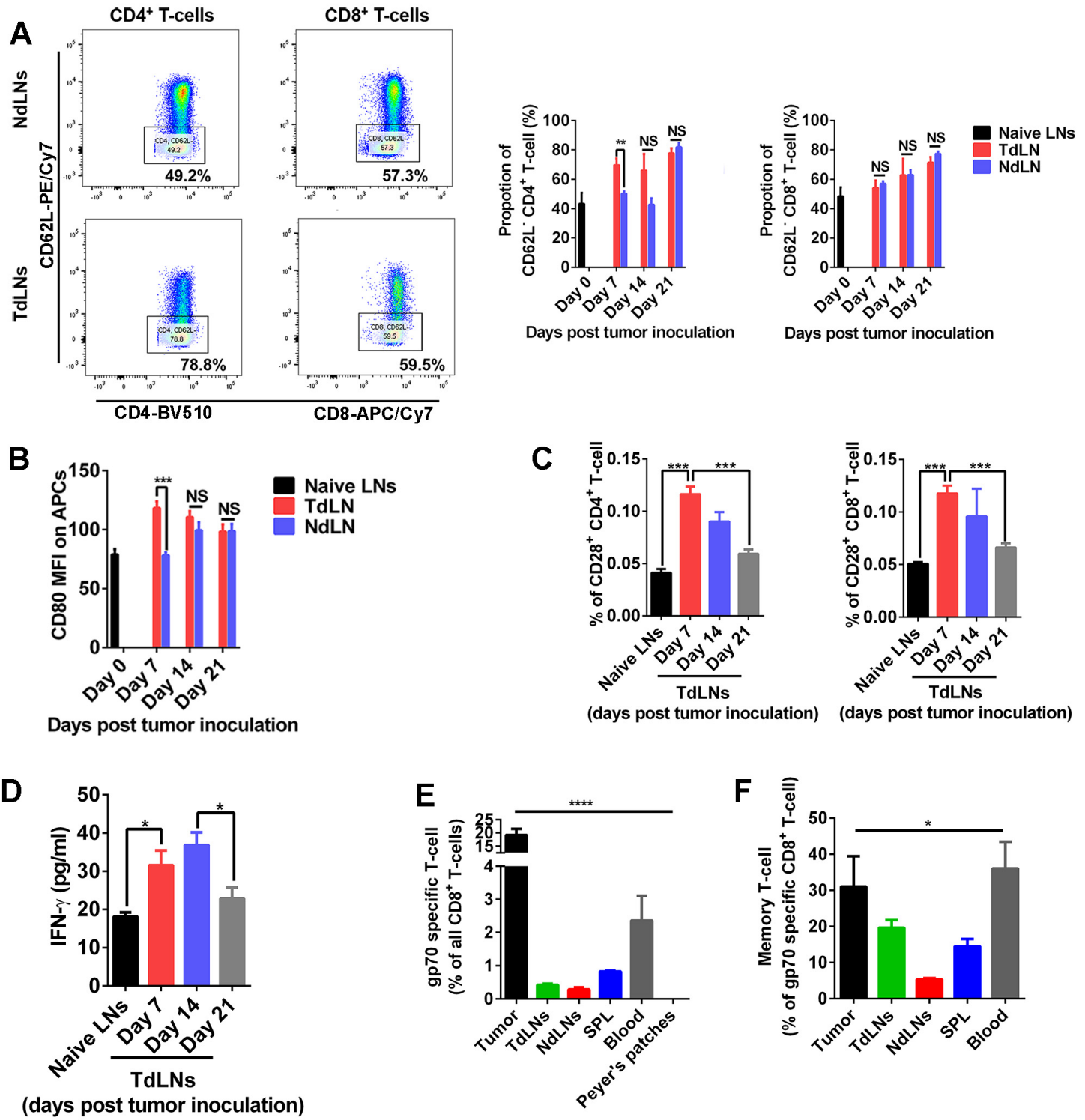
B



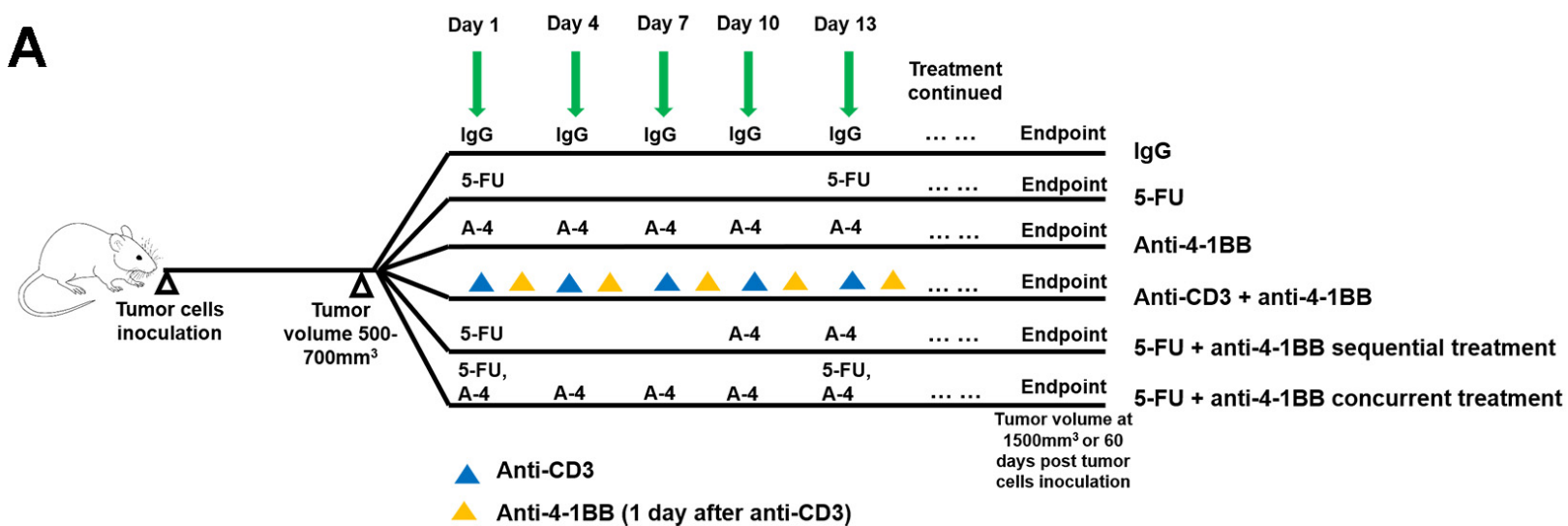
C



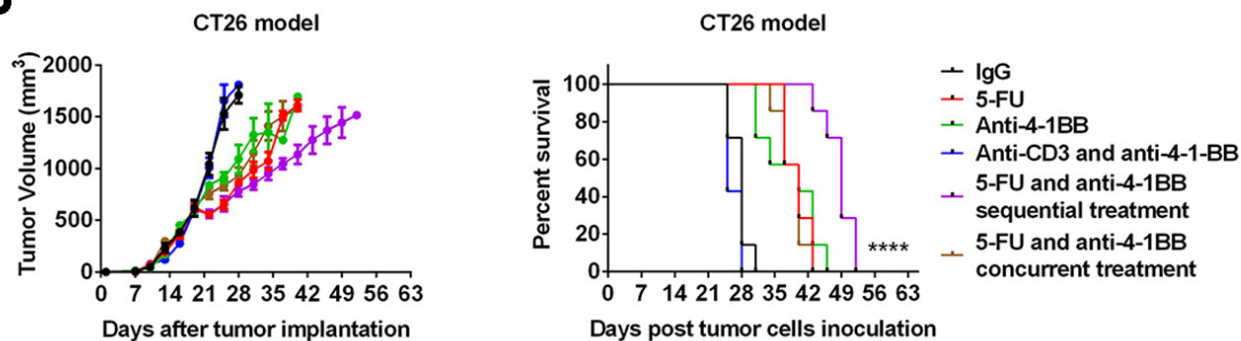




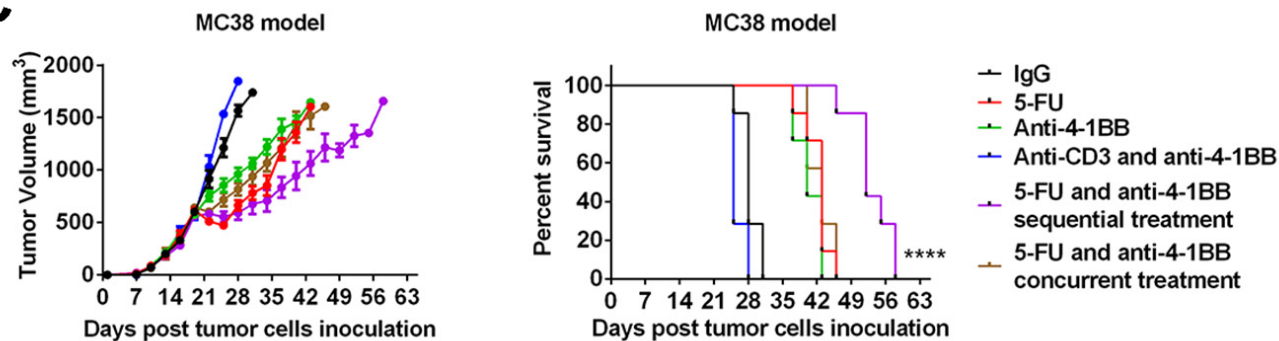
A



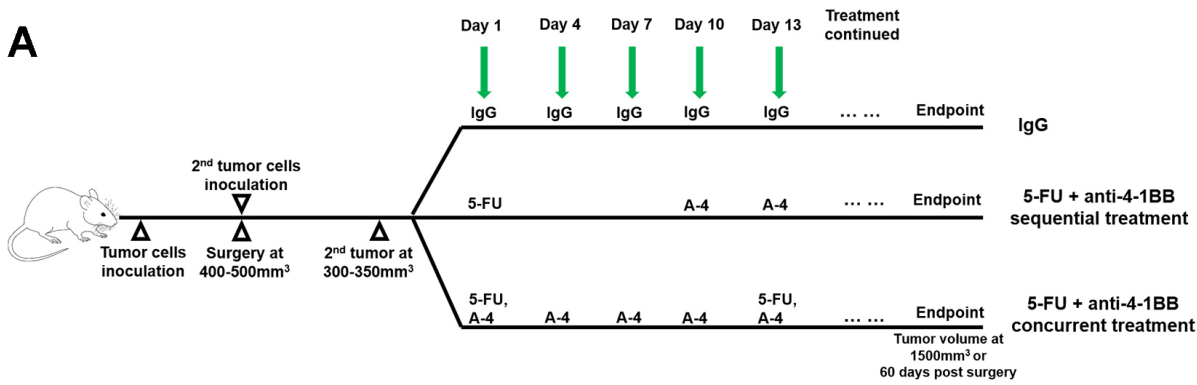
B



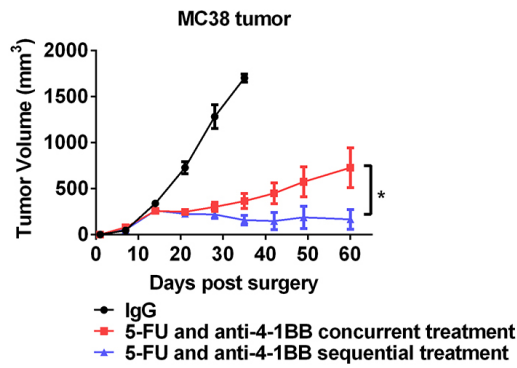
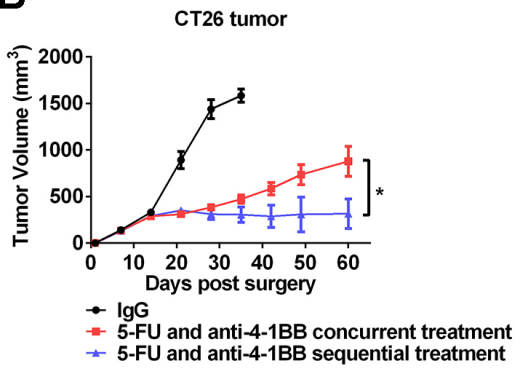
C



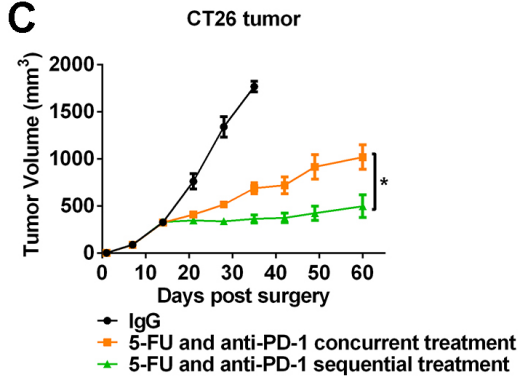
A



B

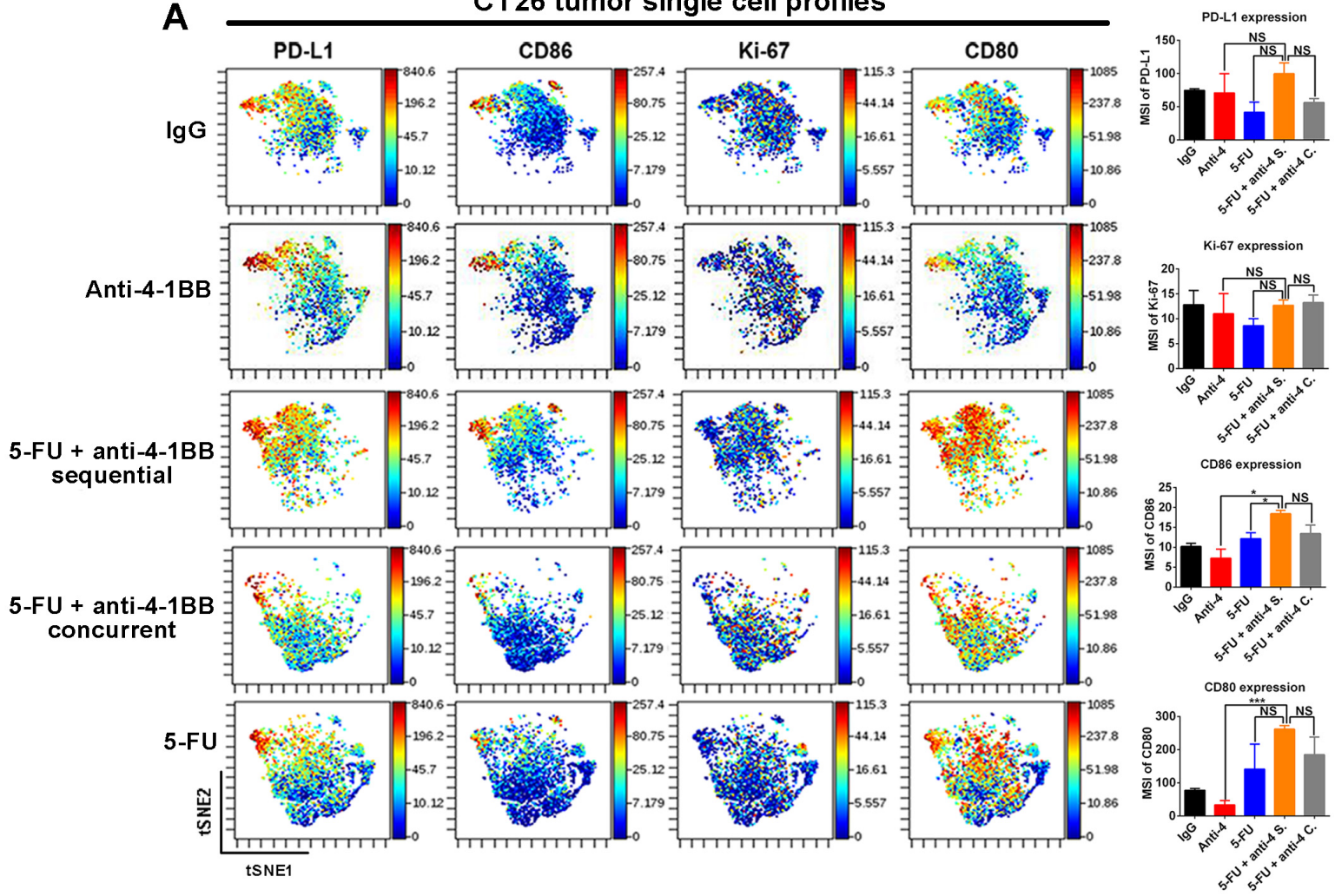


C

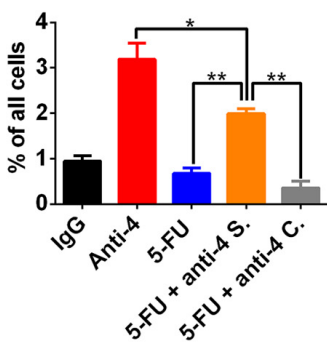


CT26 tumor single cell profiles

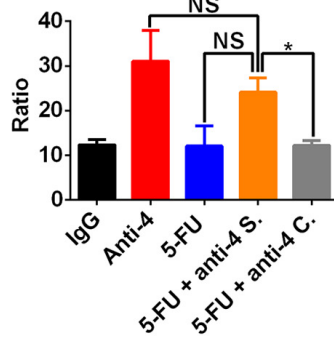
A



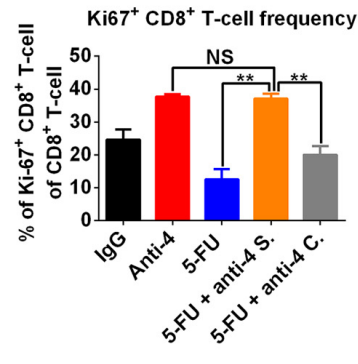
B T-cell frequency



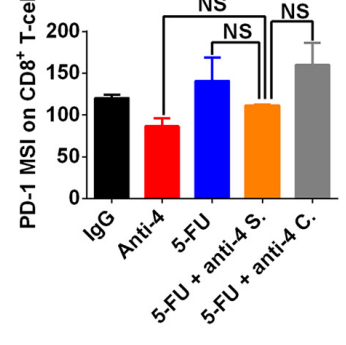
C CD8/Treg ratio



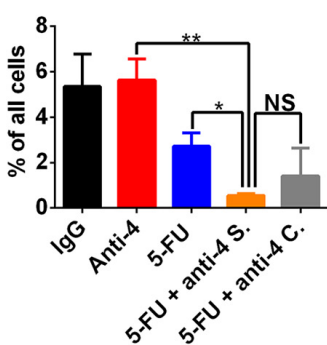
D



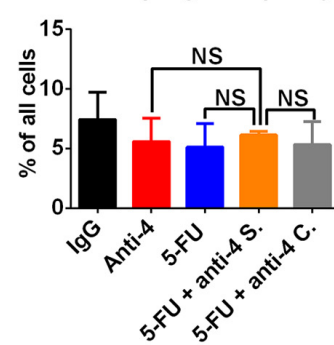
E PD-1 expression



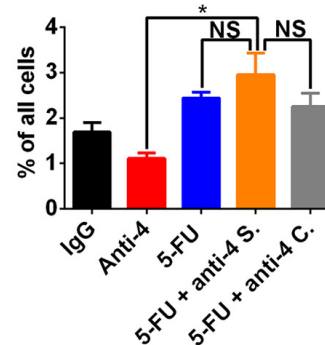
F MDSCs frequency



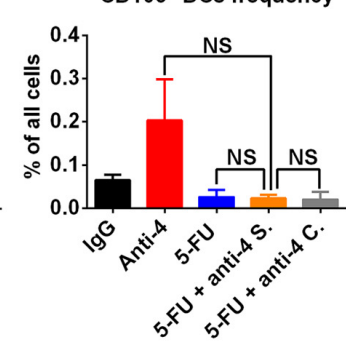
G Macrophages frequency



H NK cells frequency



I CD103+ DCs frequency



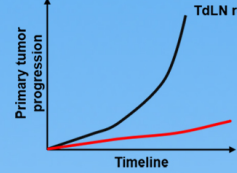
Cancer immune checkpoint
blockades therapy



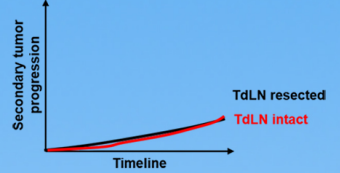
Influenced by TdLNs
resection?

Influenced by chemotherapy
combination sequence?

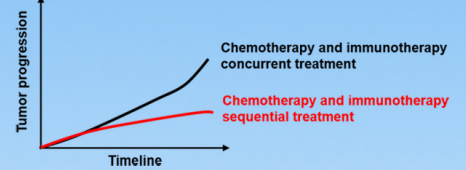
TdLNs resection before
tumor establishment



TdLNs resection after
tumor establishment



Chemotherapy and immunotherapy
combination



Cytotoxic chemotherapy that suppresses immune response
may attenuate immunotherapy efficacy when combined concurrently